Science of the Total Environment 692 (2019) 660–668

Contents lists available at ScienceDirect

Science of the Total Environment

journal homepage: www.elsevier.com/locate/scitotenv

Adsorption, aggregation and sedimentation of titanium dioxide nanoparticles and nanotubes in the presence of different sources of humic acids

Tianhui Zhao [a,b], Mengyuan Fang [b,c], Zhi Tang [b,*], Xiaoli Zhao [b], Fengchang Wu [b], John P. Giesy [d,e]

[a] College of Water Sciences, Beijing Normal University, Beijing 100875, China
[b] State Key Laboratory of Environmental Criteria and Risk Assessment, Chinese Research Academy of Environmental Sciences, Beijing 100012, China
[c] Faculty of Environmental Science and Engineering, Kunming University of Science and Technology, Kunming, Yunnan 650550, China
[d] Department of Veterinary Biomedical Sciences and Toxicology Centre, University of Saskatchewan, Saskatoon, Saskatchewan, Canada
[e] Department of Environmental Science, Baylor University, Waco, TX, United States

HIGHLIGHTS

- The adsorption amount of HA on TiO_2 NMs decreases with pH increasing, the adsorption percentages of HA_E was higher than HA_S
- The morphology of TiO_2 NMs and the source of HA have great influence on the adsorption of HA on the surfaces of TiO_2 NMs
- The suspension performance of TiO_2 NPs and TiO_2 NTs also increased by adsorbed HA
- Aromatic- rich HA was found to have a greater stabilizing effect on TiO_2 NMs than aliphatic-rich HA

GRAPHICAL ABSTRACT

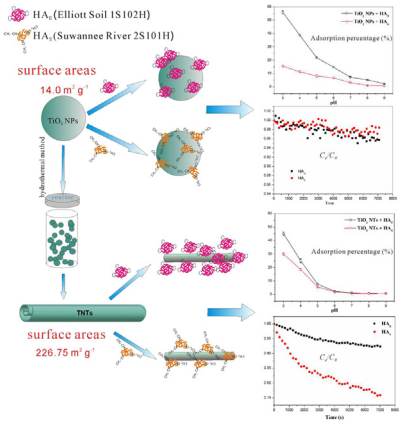

ARTICLE INFO

Article history:
Received 27 May 2019
Received in revised form 18 July 2019
Accepted 19 July 2019
Available online 20 July 2019

Editor: Dr. Jay Gan

Keywords:
Adsorption
Aggregation
Sedimentation
Titanium dioxide nanoparticles

ABSTRACT

Environmental behavior, bioavailability and risks posed by TiO_2, nanomaterials (TiO_2 NMs) in surface waters are affected by morphologies of the particles and geochemistry, including pH, inorganic and organic matter. Here, the adsorption, aggregation and sedimentation of TiO_2 nanoparticles (TiO_2 NPs) and nanotubes (TiO_2 NTs) were investigated in the presence of Elliott Soil humic acid (HA_E) and Suwannee River humic acids (HA_S). The adsorption amount of HA on TiO_2 NMs was inversely proportional to pH of solution. Maximum adsorption amount of HA on the surface of TiO_2 NMs follows the order TiO_2 NPs + HA_E (236.05 mg/g) > TiO_2 NTs + HA_E (146.05 mg/g) > TiO_2 NTs + HA_S (70.66 mg/g) > TiO_2 NPs + HA_S (37.48 mg/g). Stability of TiO_2 NPs and TiO_2 NTs largely depended on their isoelectric point, morphology and solution pH in the absence of HA. Dispersion of TiO_2 NMs was enhanced with solution pH deviated from the isoelectric point of nanomaterials due to electrostatic repulsion. Moreover, tubular structures of TiO_2 NTs with higher length-diameter ratio seem to aggregate more easily than dose sphere-like TiO_2 NPs. This might be due to their spherical structure enhancing steric repulsion. Notably, the adsorption of HA led to disagglomeration and significant stability of TiO_2 NPs and TiO_2 NTs due to steric hindrance

* Corresponding author.
E-mail address: tzwork@hotmail.com (Z. Tang).

https://doi.org/10.1016/j.scitotenv.2019.07.312

Nanotubes
Humic acid

under varying solution pH. In addition, adsorption time, concentration and sources of HA also influenced suspension/sedimentation behavior of TiO_2 NPs and TiO_2 NTs, and aromatic-rich HA_E stabilized TiO_2 NMs suspension more aggressively than aliphatic-rich HA_S.

1. Introduction

Titanium dioxide nanomaterials (TiO_2 NMs) are characterized by high chemical stability, thermal stability, resistance to corrosion and catalytic properties. These properties of TiO_2 NMs promoted them widely used in dyes, food packaging materials, environmental purification, wastewater treatment, sensors, solar cells, aerospace and other industries (Chen and Mao, 2007; Ji et al., 2014; Mondal et al., 2011; Oberdoester, 2010; Supha et al., 2015). As nanotechnology advances, TiO_2 NMs with various morphologies and functions have been created. For example, titanium dioxide nanotubes (TiO_2 NTs) have greater specific surface area than titanium dioxide nanoparticles (TiO_2 NPs), which are widely used in biomedical coatings (Cheng et al., 2018), photocatalysis (Macak et al., 2010), solar cells (Han et al., 2012; Roy et al., 2011; Shankar et al., 2009) and electrochromic devices (Koo et al., 2017). Due to their large-scale production and application, TiO_2 NMs inevitably released into the environment and participates in the geochemical cycle. It has been estimated that in Asia 42,202–44,032 metric tons of TiO_2 NMs have been released to air, water, soil, and landfills, and TiO_2 NMs rank first among commonly used engineering nanomaterials (Keller and Lazareva, 2014; Hochella et al., 2019).

TiO_2 NMs are nonbiodegradable so they can accumulate in the environment and can damage ecosystems and pose risks to human health through the food chain (Forgacs et al., 2004). TiO_2 NMs have significant effect on the unicellular green alga *Chlamydomonas reinhardtii* (Wang et al., 2008), the mortality of large flea (Lovern and Klaper, 2010) and respiratory system of rainbow trout (Federici et al., 2007). Moreover, the suspension/sedimentation and morphology of TiO_2 NMs in aqueous environments significantly affect their toxicity to aquatic organisms (Sendra et al., 2017). The results of previous study demonstrated that the TiO_2 NMs treated by filtration are more toxic to large fleas than sonication (Hillegass et al., 2010). In natural waters, complex physical and chemical parameters, such as pH, temperature, natural organic matter and ionic strength influence the migration, transformation and suspension/sedimentation of TiO_2 NMs (Wang et al., 2012). To this end, studying the suspension/sedimentation behavior of TiO_2 NMs in water could provide theoretical basis for understanding their biological toxicity and ecological effects.

Humic acid (HA), an important component of dissolved organic matter (DOM), has been used to evaluate its environmental geochemical processes (Erhayem and Sohn, 2014b). Sources of HA in water are mainly divided into those that are endogenous and exogenous. Endogenous HA is mostly generated from animal and plant residues in water through long-term physical, chemical and biological interactions. In contrast, exogenous HA is primarily produced from surface water dissolving the HA in soil. HA derived from different sources has large differences in molecular weight, elemental composition and functional groups (carboxyl groups, phenols and carbonyl amine groups), which will strongly affect its adsorption and complexation with metals and organic pollutants in water, and thus affects their migration, transformation and fate (Erhayem and Sohn, 2014b; Lin et al., 2012; Mcdonald et al., 2004; Schnitzer and Khan, 1974; Sun et al., 1997). Therefore, it is still urgent to investigate the effects of HA from different sources on the environmental behavior of nanomaterials.

The results of previous studies have indicated that the adsorption of HA can affect the suspension/sedimentation and ecotoxicity of TiO_2 NPs (Dasari and Hwang, 2010; Lee et al., 2011; Thio et al., 2011). The adsorption of HA on TiO_2 NPs was through electrostatic adsorption and ligand exchange between the surface hydroxyl groups of TiO_2 NPs and carboxyl groups or phenolic hydroxyl groups of HA molecules (Erhayem and Sohn, 2014b; Li et al., 2015). Compared to TiO_2 NPs, TiO_2 NTs differ in terms of physicochemical properties such as isoelectric point, specific surface area, active site and surface functional groups (Liu et al., 2005; Shankar et al., 2009), and the unique physical and chemical properties of TiO_2 NTs further give rise to a greater adsorption capacity, and their ability to adsorb pollutants in water is also stronger (Xiong et al., 2011). Moreover, the suspension/sedimentation properties of TiO_2 NPs and TiO_2 NTs in water are different. Compared with TiO_2 NTs, TiO_2 NPs are more stable in natural waters due to their micro-structure (Bavykin et al., 2006; Chen et al., 2010; Niu et al., 2009). Results of previous studies have indicated that HA promotes the suspension of TiO_2 NPs in water due to electrostatic repulsion and steric hindrance (Chowdhury et al., 2012; Erhayem and Sohn, 2014b; Li et al., 2015). However, limited research about effects of HA on the suspension/sedimentation properties of TiO_2 NTs. Liu et, al. studied the effects of HA derived from water, pH and ionic strength on the aggregation, suspension and sedimentation of TiO_2 NTs (Liu et al., 2013). Nonetheless, these studies did not compare effects of sources of HA on the suspension/sedimentation of TiO_2 NTs. Indeed, it is important to understand the adsorption of different sources of HA on the surfaces of TiO_2 NPs and TiO_2 NTs, and effects of HA on aggregation and suspension/sedimentation.

By comparing two different sources of HA, this study systematically investigates their adsorption on surfaces of the TiO_2 NPs and TiO_2 NTs, and the effects on suspension/sedimentation properties of TiO_2 NMs. This investigation would provide the theoretical basis for recognizing the environmental behaviors and potential ecological risks of TiO_2 NMs with different morphologies in the presence of either of several sources of HA.

2. Experimental and method

2.1. Materials and chemicals

TiO_2 NPs used in this experiment were purchased from J&K Scientific (San Jose, USA, CAS: 13463-67-7). HA Elliott Soil (1S102H, HA_E) and HA Suwannee River (2S101H, HA_S) were purchased from the International Humic Substances Society (IHSS, St. Paul, USA). The element constitution, amount of acid functional groups and the corresponding distribution of organic carbon based on the spectra of ^{13}C NMR of HA_E and HA_S are listed in Table S1. All the chemicals used in the experiments were analytical reagent grade unless otherwise specified, and they were used without further purification. Ultra-pure Milli-Q water (18.2 MΩ cm) produced by a Milli-Q Advantage System (Merck, Darmstadt, Germany) was used for all experiments. All statistical analysis was performed in Origin Pro 8.0.

2.2. Preparation of HA stock solutions

HA was dissolved in 0.1 M NaOH solution. The solution was kept in a shaker at room temperature (22 ± 1 °C) for 12 h to dissolve completely, then filtered through a 0.45 μm fiber membrane (MF Cat No: HAWP04700) prior to use. The HA stock solution was diluted in a series of concentrations ranging from 10 to 60 mg/L. The pH of each HA solution was adjusted to the desired value by adding NaOH and HCl solution.

2.3. Preparation of protonated TiO_2 NTs

TiO_2 NTs were prepared by using the alkaline hydrothermal method as previously described (Zhao et al., 2019). First, 3 g of anatase-phase TiO_2 NPs powder was dispersed in 100 mL of 10 M NaOH solution and vigorously stirred for 24 h. Subsequently, the mixture was autoclaved at 150 °C for 24 h. The obtained white product was washed with deionization water until the supernatant pH became neutral, and then soaked in 0.5 M hydrochloric solution for 5 h. Interlayer sodium ions were anticipated to be exchanged for protons during the soaking of the nanotubes in acidic solution. Then, the protonated TiO_2 NTs were again washed to pH 7 with deionized water. Finally, the products were dried at 90 °C.

2.4. Batch adsorption experiments

All batch tests were performed in 100 mL glass bottles by adding 10 mg (dry mass) of TiO_2 NP or TiO_2 NT adsorbent to HA solutions. The final volume of mixture was 50 mL. The solution pH was adjusted by adding 0.1 M HCl or NaOH. Ionic strength was controlled to 0.01 M with 1 M NaCl solution.

To investigate effect of pHs on adsorption, a series of suspension samples were prepared by adding TiO_2 NMs to HA solution (40 mg/L) and adjusting each mixture to pH 3.0, 4.0, 5.0, 6.0, 7.0, 8.0, 9.0 or 10.0, respectively. The mixture was stirred for 24 h, then the supernatant was filtered through 0.45 μm pore-size cellulose, and absorbance was measured using a UV–Vis spectrophotometer at 254 nm (UV-8453, Agilent, Santa Clara, USA).

Adsorption isotherms were developed from data collected by adding TiO_2 NMs to various initial concentrations of HA (5, 10, 20, 30, 40, 50 or 60 mg HA/L). The mixture was stirred on a rotary shaker for 24 h. Then the supernatant was filtered through 0.45 μm pore-size cellulose prior to absorbance measurement using a UV–Vis spectrophotometer at 254 nm. The adsorption isotherms were fitted using both Langmuir and Freundlich adsorption isotherm models.

Adsorption kinetics were determined by adding TiO_2 NMs to an initial HA concentration of 20 mg/L measured after various durations. The pH of the suspension was adjusted to 3.0 ± 0.1. The suspension was stirred in a shaker. A series of samples were prepared by separating the supernatant from each suspension by a magnet after 0, 1, 2, 4, 8, 12, 24, 48 or 96 h, filtered through a 0.45 μm glass fiber membrane. Change in the absorbance of each supernatant sample was analyzed using a UV–Vis spectrophotometer at 254 nm.

2.5. Aggregation/sedimentation of TiO_2 NMs and TiO_2 NMs/HA

The change of TiO_2 NMs intensity-weighted averaged hydrodynamic diameter (D_h) over time (t) was measured using time-resolved dynamic light scattering (TR-DLS) (Nano-ZS90 Zetasizer, Malvern, United Kingdom). The mixture was transferred immediately into a cuvette and measured by use of DLS. Each measurement lasted for 60 s, numbers of measurement of each sample were 240. The sedimentation of TiO_2 NMs in each suspension was evaluated by measuring the absorbance at 508 nm using a UV–Vis spectrophotometer (Li et al., 2015). The ratio of absorbance C_e measured at multiple intervals in respect to the initial absorbance C_0 was calculated. A low ratio indicated that more TiO_2 NMs had been accumulated, and this is proportional to the probability of sedimentation having occurred.

2.6. Characterization

The morphology of TiO_2 NPs and TiO_2 NTs were determined by transmission electron microscopy (TEM), H7500 transmission electron micrograph (Hitachi, Japan) operating at 120 kV. Specific surface areas (BET) of samples were investigated using an F-Sorb 3400 automatic surface area Gold APP Instrument. Zeta potentials of all samples were determined with Nano-ZS90 Zetasizer.

3. Results and discussion

3.1. Characterization of TiO_2 NPs and TiO_2 NTs

The mean particle size of TiO_2 NPs was approximately 25 nm. The outer and inner diameter of TiO_2 NTs was about 9–10 nm and 1–2 nm, respectively. While the length of TiO_2 NTs was about 0.1–0.2 μm, the diameter and length of TiO_2 NTs were relatively uniform (Fig. 1). The specific surface areas of TiO_2 NPs and TiO_2 NTs was 14.0 and 226.75 m^2/g, respectively, which was greater than formerly due to a reduction in dimensionality causing a significant increase in specific surface area during TiO_2 NTs synthesis (Roy et al., 2011). After being immersed in HCl solution (remove the sodium ions in the crystal lattice), TiO_2 NTs synthesized by concentrated alkaline hydrothermal process can form a tubular structure. Importantly, the calcination temperature determines the diameter of the tube (Kasuga, 2006; Wang et al., 2002).

Zeta potentials of TiO_2 NPs and TiO_2 NTs varied with pH of the solution. When pH was approximately 2.0, the Zeta potential of TiO_2 NPs was positive and reached the maximum. Zeta potential of TiO_2 NPs was inversely proportional to pH. When the pH was approximately 6.2, Zeta potential of TiO_2 NPs was zero. With pH continued to increase, the Zeta potential value tend to become more negative. These results suggest that the isoelectric point of TiO_2 NPs was approximately 6.2, whilst the Zeta potential of TiO_2 NTs decreased with pH increasing, the Zeta potential of TiO_2 NTs declined to zero at pH = 3.2, which was significantly lower than TiO_2 NPs. This is due to the deprotonation of the surface hydroxyl groups during the synthesis of TiO_2 NTs (Niu et al., 2009).

3.2. Adsorption study

3.2.1. Effect of pH on the adsorption of different sources of HA on the surface of TiO_2 NPs and TiO_2 NTs

In aqueous environments, pH determines surface charges of nanoscale metal oxides. Adsorption amount of HA_E and HA_S on the surfaces of TiO_2 NPs and TiO_2 NTs decreased with increasing pH (Fig. 2). Maximum adsorption percentage of HA on TiO_2 NPs and TiO_2 NTs was achieved at pH = 3.0, the adsorption percentage of TiO_2 NPs to HA_E and HA_S was 55.9% and 15.5%, respectively, and the adsorption percentage of TiO_2 NTs to HA_E and HA_S are 45.0% and 30.0%, respectively. This is because when pH is less than the isoelectric point of TiO_2 NMs, their surfaces are positively charged ($Ti\text{-}OH + H^+ \Leftrightarrow Ti\text{-}OH_2^+$). Conversely, when pH is greater than the isoelectric point, the surfaces are negatively charged ($Ti\text{-}OH \Leftrightarrow Ti\text{-}O^- + H^+$ or $Ti\text{-}OH + OH^+ \Leftrightarrow Ti\text{-}O^- + H_2O$) (Zhao et al., 2019; Kataoka et al., 2004). Therefore, adsorption of negatively charged HA on surfaces of TiO_2 NMs is strongly affected by the pH of the solution. When pH = 3.0, the positive charge density on surfaces of TiO_2 NMs was largest, so the adsorption amount of HA_E and HA_S reached the maximum. When pH > 8.0, the adsorption percentage of HA_E and HA_S on the surface of TiO_2 NPs was close to zero. For TiO_2 NTs, the adsorption percentage decreased significantly when pH > 6.0. This is due to the difference in isoelectric points between TiO_2 NPs and TiO_2 NTs. The surface of TiO_2 NTs contains a large number of –OH functional groups, which results in their isoelectric point being less than that of TiO_2 NPs (Niu et al., 2009). As the pH of the solution increased, the positive charge density on the surface of TiO_2 NMs decreased. Accordingly, the adsorption amount of HA on the surface of TiO_2 NMs through electrostatic adsorption decreases continuously. When the pH of the solution was higher than the isoelectric point of TiO_2 NMs, the surface was negatively charged, therefore, the adsorption of HA_E and HA_S by electrostatic attraction was hindered.

For different sources of HA, the adsorption percentage of HA_E on TiO_2 NPs and TiO_2 NTs were greater than that of HA_S at the same solution pH

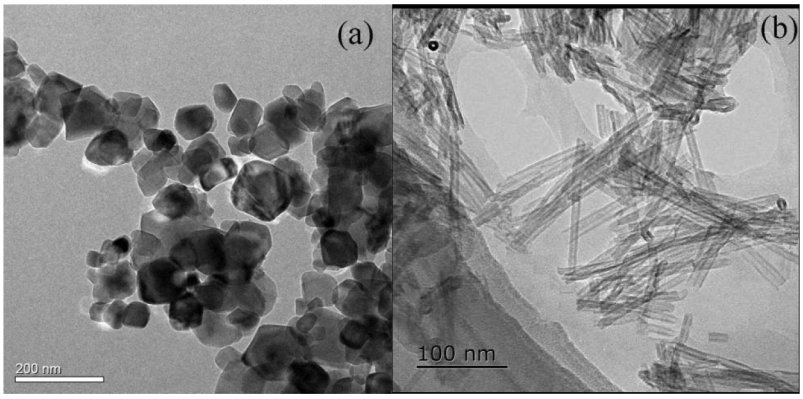

Fig. 1. Transmission electron microscope pictures of TiO_2 NPs (a) and TiO_2 NTs (b).

value. Due to containing more aromatic functional groups, HA_E has a more hydrophobic effect than HA_S (Table S1), which can promote its adsorption on nano-materials (Erhayem and Sohn, 2014a, 2014b). The adsorption percentage of HA_E on surfaces of TiO_2 NTs was less than that on surfaces of TiO_2 NPs. This is because the isoelectric point of TiO_2 NTs is less, and the positive charge density on surfaces of TiO_2 NPs is greater than that of TiO_2 NTs at the same pH. Therefore, adsorption percentage of HA_E on TiO_2 NPs was greater than that on TiO_2 NTs. For HA_S, the adsorption percentage was greater on the surface of TiO_2 NTs. HA_S contain more acidic functional groups (such as carboxyl groups, Table S1), which will enter into ligand exchange reactions with function groups on the surfaces of TiO_2 NMs (Li et al., 2015). HA_S contains more aliphatic components, so it is more curled under acidic conditions and which might hinder continued adsorption of HA_S. Therefore, the adsorption amount of HA_S on the TiO_2 NTs was greater than TiO_2 NPs, and the specific surface area of TiO_2 NMs plays a major role.

3.2.2. Adsorption isotherm

Adsorption isotherms of HA_E or HA_S on TiO_2 NMs were compared (Fig. S2). Both the Langmuir (Eq. (1)) and Freundlich (Eq. (2)) isotherms fitted the data well.

$$q_e = \frac{q_m k_L C_e}{1 + k_L C_e} \quad (1)$$

$$q_e = k_F C_e^{1/n} \quad (2)$$

where: q_e is the amount (mg/g) of adsorbed HA at equilibrium and, Ce is the equilibrium HA concentration (mg/L) in solution. q_m (mg/g) represents the maximum adsorption capacity; k_L (L/g) is the Langmuir equilibrium constant; In Eq. (2), k_F ($mg^{1-(1/n)}$ $L^{1/n}$/g) and n are the Freundlich parameters.

The Langmuir and Freundlich parameters (Table S2) show that adsorption of HA_E and HA_S on surfaces of TiO_2 NPs is more consistent with Langmuir fitting, the adsorption of HA_S on the surface of TiO_2 NTs was more consistent with Freundlich fitting. These results indicate that adsorption of HA_E and HA_S on TiO_2 NPs and HA_E on TiO_2 NTs was more inclined to be monolayer adsorption. In contrast, HA_S adsorbed on TiO_2 NTs might favor multilayer adsorption (Zou et al., 2016). The maximum adsorption amount of HA on the surface of TiO_2 NMs follows the order TiO_2 NPs + HA_E (236.05 mg/g) > TiO_2 NTs + HA_E (146.05 mg/g) > TiO_2 NTs + HA_S (70.66 mg/g) > TiO_2 NPs + HA_S (37.48 mg/g) (Table S2). It can be seen that the adsorption amount of HA_E was larger than that of HA_S on the same kind of TiO_2 NMs. For the same kind of HA, the adsorption amount of HA_E on the surface of TiO_2 NPs was larger than that on TiO_2 NTs. Consistent with above results, the adsorption amount of HA_S on TiO_2 NTs was larger.

3.2.3. Adsorption kinetics

Adsorption kinetics is key to understanding and predicting environmental behavior of TiO_2 NMs in aqueous environments. At pH = 3.0, the maximum adsorption amount of HA_E and HA_S on TiO_2 NPs was reached after approximately 20 h and declined thereafter. Adsorption reached steady state after 40 h (Fig. 3a and b). When the pH was 3.0, adsorption of HA_E and HA_S on TiO_2 NTs reached the maximum adsorption amount after about 24 h (Fig. 3c and d). However, the difference in adsorption between HA_E and HA_S on the surfaces of TiO_2 NMs was large. Maximum adsorption amount of HA on TiO_2 NMs can reach 60.7 mg/g (HA_E on TiO_2 NPs), 28.5 mg/g (HA_S on TiO_2 NPs), 44.0 mg/g (HA_E on TiO_2 NTs), 27.2 mg/g (HA_S on TiO_2 NTs) (Fig. 3), and this order was consistent with the above research results. The main reason for this phenomenon may be HA of various sources have different existential state when the pH was 2.0–3.0, which would cause a difference in ductility and even affect the adsorption rate of HA on surfaces of TiO_2 NMs.

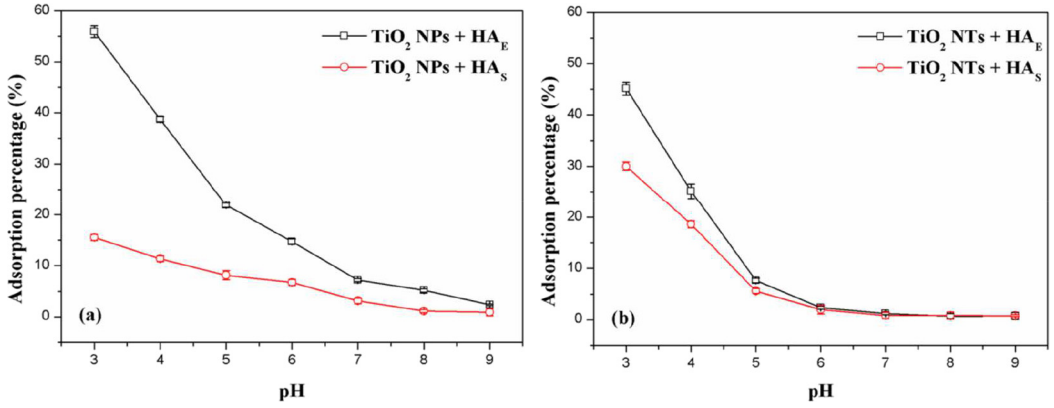

Fig. 2. Effect of different pH values of solution on the adsorption of different sources of HA (HA_E, HA_S) on TiO_2 NPs (a) and TiO_2 NTs (b).

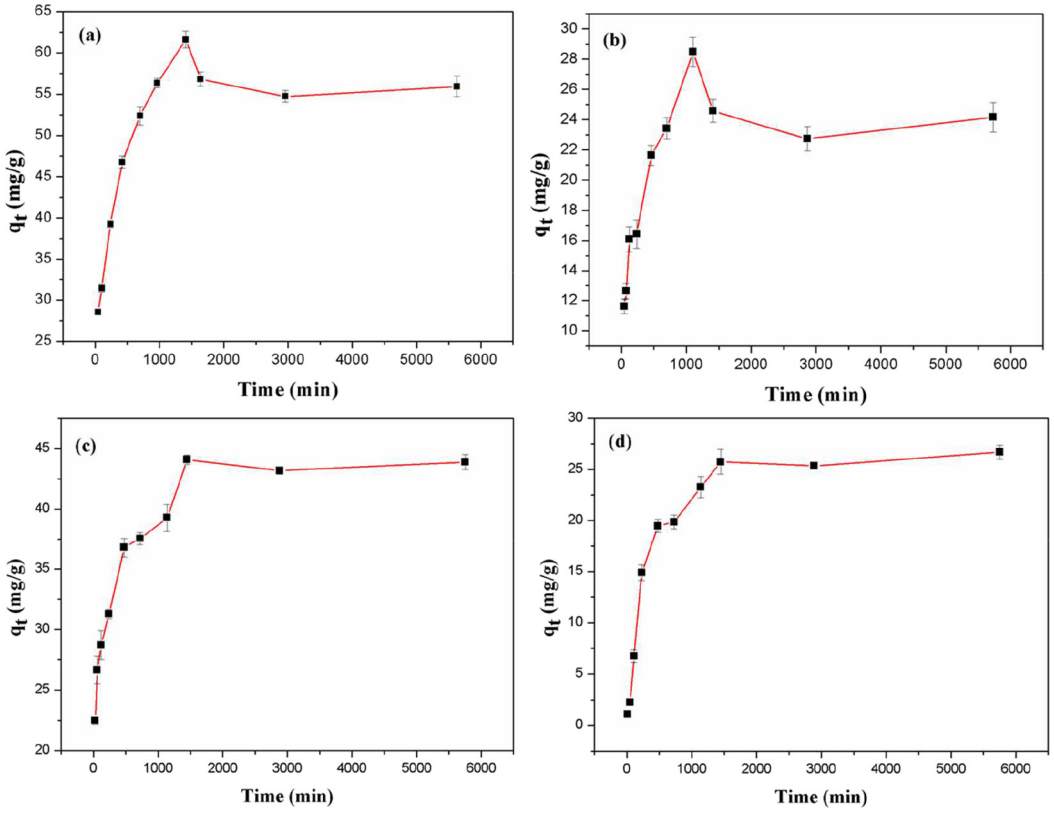

Fig. 3. The adsorption amount of HA_E (a) and HA_S (b) on TiO_2 NPs, the HA_E (c) and HA_S (d) on TiO_2 NTs at different reaction times.

Adsorption kinetic parameters can be determined by measuring the adsorption rate of HA on TiO_2 NMs and using the first-order (Eq. (3)) and second-order kinetic equations (Eq. (4)) to produce the fit.

$$\text{Pseudo-first-order model } q_t = q_e\left(1-e^{-k_1 t}\right) \tag{3}$$

$$\text{Pseudo-second-order model } \frac{t}{q_t} = \frac{1}{k_2 {q_e}^2} + \frac{1}{q_e}t \tag{4}$$

where: k_2 is the rate constant of adsorption (in g/mg/min); q_t is the amount of HA adsorbed by adsorbent at any time (mg/g); q_e is equilibrium adsorption capacity (mg/g). Initial sorption rate, h_o (mg/g/min) can be defined as follow (Eq. (5)):

$$h_o = k_2 {q_e}^2 (t \to 0) \tag{5}$$

Both k_2 and h_o can be determined experimentally by plotting of t/q_t against t.

For adsorption of HA_E and HA_S on TiO_2 NPs and HA_E on TiO_2 NTs, the results demonstrate that the fitting using pseudo second-order kinetics were all better (with a higher R^2) than pseudo first-order fitting (Table S3). This indicates that chemisorption is the main factor affecting the adsorption rate. For the adsorption of HA_S on the surfaces of TiO_2 NTs, the fitting effect of pseudo first-order was slightly better than that of pseudo second-order. This means that both chemical and physical adsorption processes were involved in the adsorption of HA_S on TiO_2 NTs. This is consistent with the results of the previous adsorption isotherms. From the value of h_0, the initial reaction rate of HA adsorption on the surfaces of two nano-materials follows the order TiO_2 NPs + HA_E > TiO_2 NPs + HA_S > TiO_2 NTs + HA_E > TiO_2 NTs + HA_S. The adsorption amount of HA_E on the surface of two nano-materials after adsorption equilibrium were larger than that of HA_S. The adsorption amount of HA_E on the surface of TiO_2 NPs was greater than TiO_2 NTs, but the result was opposite for HA_S. This mainly because the adsorption experiments were conducted under acidic conditions, the density of the positive charge on the surface of TiO_2 NPs was higher than that of TiO_2 NTs, thus leading to stronger electrostatic interaction with HA. In addition, the initial reaction rate of HA_E adsorbed on TiO_2 NMs was always greater than HA_S due to the greater hydrophobicity of HA_E result in a greater affinity to TiO_2 NMs (Erhayem and Sohn, 2014a).

3.3. Sedimentation study

3.3.1. Effect of pH on suspension/sedimentation properties of TiO_2 NPs

The suspension performance of TiO_2 NPs in relation to pH followed the order pH = 9.0 > pH = 3.0 > pH = 7.0 > pH = 5.0, while the suspension performance of TiO_2 NPs followed the order pH = 9.0 > pH = 7.0 > pH = 5.0 > pH = 3.0 (Fig. 4). This difference might be related to the respective isoelectric points of TiO_2 NPs and TiO_2 NTs. In this study, the isoelectric points of TiO_2 NPs and TiO_2 NTs were 6.2 and 3.2, respectively. When the solution pH was close to their isoelectric point, the surface potential of the material will be close to zero, and the aggregation and sedimentation of nanoparticles were likely to occur. This is because of the electrostatic repulsion effect between the particles weakens and the intermolecular force increases (Zhang et al., 2009).

As HA adsorbed on the surfaces of TiO_2 NMs, the suspension performance of TiO_2 NPs and TiO_2 NTs also increased, particularly in the case of HA_E on TiO_2 NPs, which was due to adsorption between the TiO_2 NMs and the HA is generated through electrostatic interaction, hydrophobic interaction, complexation-ligand exchange. When HA adsorbed on the surface of the TiO_2 NMs, HA not only increased the density of surface charge but also the energy barrier between particles by steric hindrance (Liu et al., 2013), which is consistent with previous studies (Li et al., 2015; Pan and Xing, 2008). Moreover, sphere-like TiO_2 NPs agglomerates seem to more stable than TiO_2 NTs with tubular structures due to spherical structure enhancing steric repulsion (Liu et al., 2013).

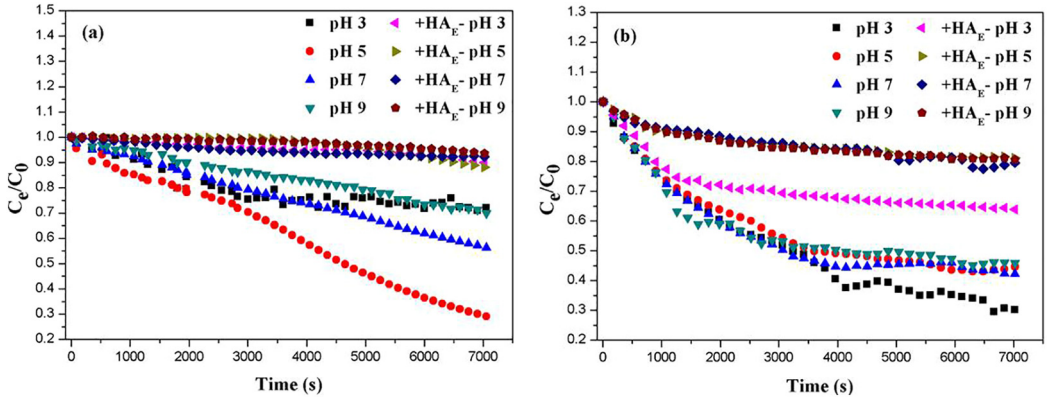

Fig. 4. Suspension/sedimentation of TiO_2 NPs (a) and TiO_2 NTs (b) prior to and after HA_E adsorbed at different solution pH values.

3.3.2. Effect of adsorption time on suspension/sedimentation performance of TiO_2 NMs

The effect of adsorption time on the suspension/sedimentation performance of TiO_2 NPs and TiO_2 NTs was studied (Fig. 5). When pH was 3.0, the suspension of TiO_2 NPs increased from 1 h to 20 h. When the reaction exceeded 24 h, the suspension property deteriorated and caused sedimentation. For TiO_2 NTs, the suspension performance increased during the initial phase, then waned after 12 h. When the reaction reached 20 h, there was no significant change in the suspension performance of TiO_2 NTs.

Changes in the suspension/sedimentation performance of TiO_2 NPs or TiO_2 NTs might be driven by the adsorption amount of HA_E during reaction time. As studying the adsorption kinetics of HA on the surface of TiO_2 NPs above, the adsorption of HA_E on the surface of TiO_2 NPs was mainly due to electrostatic interaction in the first 1 h, the negatively charged HA neutralizes the positive charge on the surface of TiO_2 NPs, which leading to TiO_2 NPs/HA complex aggregate more easily than TiO_2 NPs in absence of HA. With more HA_E adsorbed on the surface TiO_2 NPs by hydrophobic effect and complexation-ligand exchange, the density of surface charge of the TiO_2 NPs gradually increased, and more HA adsorbed on the surface of TiO_2 NPs would result in stronger steric hindrance. Therefore, TiO_2 NPs/HA complex were not easily to aggregate. It is worth noting that the suspension performance of TiO_2 NPs decreased when the adsorption time reached 20 h. As shown in Fig. 3a, when the adsorption time reached 24 h, the adsorption amount of HA_E on the surface of TiO_2 NPs decreased, this result may lead to a decrease of the suspension performance of TiO_2 NPs. For the suspension/sedimentation performance of TiO_2 NTs/HA_E complexes, the surface of TiO_2 NTs exhibits positive charges at pH 3.0, the negatively charged HA_E continuously adsorbed on the surface of TiO_2 NTs, neutralizing its surface charge. As such, the repulsive force and steric hindrance also increased as more HA_E adsorbed on the surface of TiO_2 NTs, then the suspension performance of nanotubes in aqueous solution increased. Therefore, the increase of adsorption amount of HA_E on surface of TiO_2 NMs with time would greatly promote stable and suspension of TiO_2 NMs under acidic conditions.

3.3.3. Effect of concentrations of HA on the suspension/sedimentation performance of TiO_2 NPs and TiO_2 NTs

As shown in Fig. 6, for TiO_2 NTs, at the solution pH = 6.5, the hydrodynamic diameter of TiO_2 NPs decreased with the increased of HA_E concentration, the TiO_2 NPs became difficult to aggregation, and suspended was maintained. For TiO_2 NTs, the hydrodynamic diameter increased slightly with the increase of HA_E concentration. When the HA_E concentration reached 20 mg/L, the TiO_2 NTs/HA_E complexes settled most readily, and at 40 mg/L, the particle size of TiO_2 NTs were relatively small resulting in a stable suspension. Comparing to TiO_2 NPs, the sedimentation rate of TiO_2 NTs was much higher than that of TiO_2 NPs in the presence of same HA concentration. This is because the isoelectric point of TiO_2 NPs was lower, the adsorption amount of HA_E adsorbed on the surface of TiO_2 NPs by electrostatic attraction was higher at pH 6.0, so the density of surface charge of TiO_2 NPs was larger, and the steric hindrance effect of HA_E was stronger. Therefore, the sedimentation performance of TiO_2 NTs was greater than TiO_2 NTs at the same concentration of HA_E.

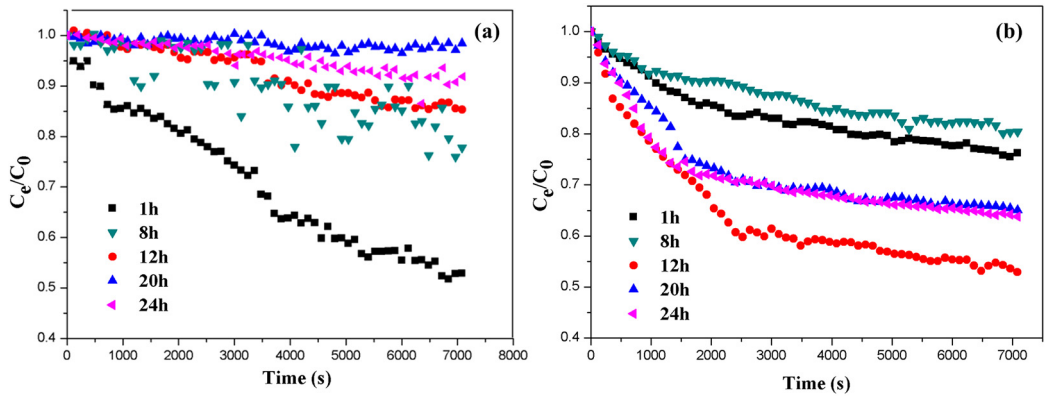

Fig. 5. Effect of adsorption time on the suspension/sedimentation of TiO_2 NPs (a) and TiO_2 NTs (b).

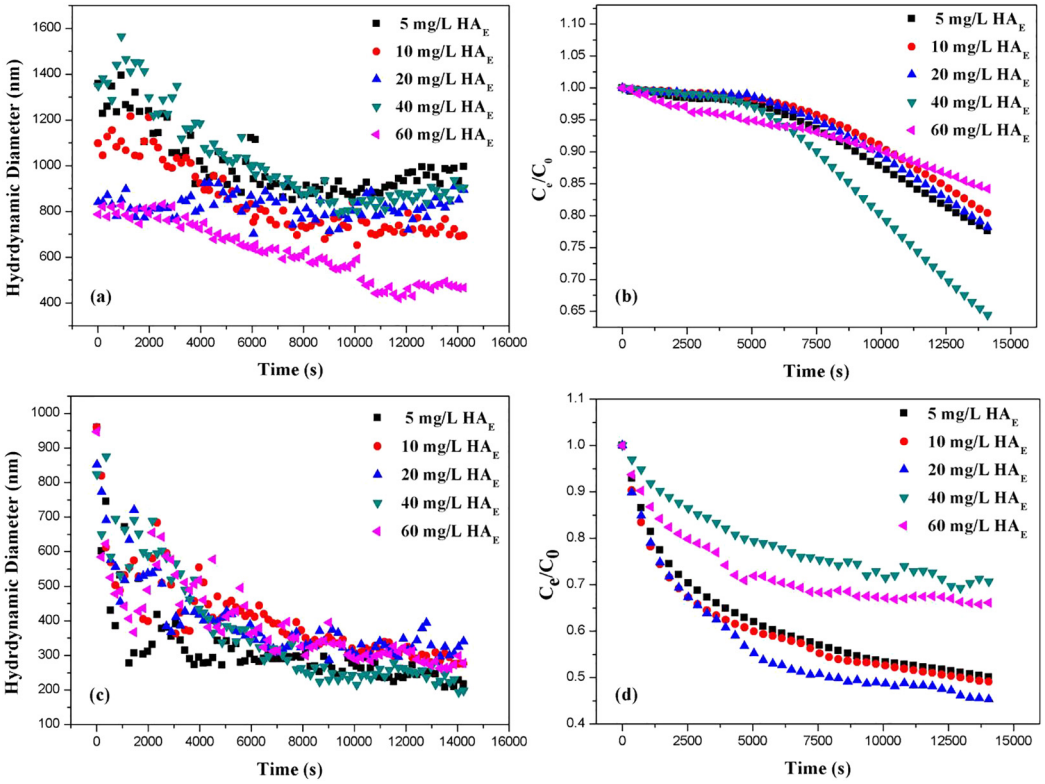

Fig. 6. The Aggregation (a) and sedimentation (b) of TiO_2 NPs, the aggregation (c) and sedimentation (d) of TiO_2 NTs at the condition of pH = 6.0.

3.3.4. Effect of sources of HA on the suspension/sedimentation performance of TiO_2 NPs and TiO_2 NTs

There were obvious differences in the chemical composition of HA obtained from different sources and different extraction methods. These fatty, aromatic, surface active component and carbohydrate structure of HA greatly influence the suspension/sedimentation performance of TiO_2 NMs (Chowdhury et al., 2012; Loosli et al., 2014), which also affects the migration, transformation and bioavailability of TiO_2 NMs in aqueous environments. Therefore, it is crucial to understand the effect of different sources of HA on the suspension/sedimentation performance of TiO_2 NPs and TiO_2 NTs.

Both HA_E and HA_S could improve the suspension performance of TiO_2 NMs, with the former having a stronger effect, especially for TiO_2 NTs (Fig. 7) due to greater adsorption amount of HA_E. Moreover, the difference in composition between HA_E and HA_S also contributed towards this phenomenon. Table S1 have shown that there was a certain difference between Aromatic/Aliphatic ratio of HA_E (3.125) and HA_S (1.069). Since HA_E contains relatively more aromatic compounds, it was more conducive to TiO_2 NMs stabilization in solution. This indicates that the stability of TiO_2 NMs in HA solution was probably related to the presence of negatively charged phenolic hydroxyl functional groups. Furthermore, HA with higher aromaticity contains higher proportion of phenolic hydroxyl carbon, which enhanced the suspension of TiO_2 NPs (Li et al., 2015; Lin et al., 2016).

4. Conclusions

Two different morphologies of TiO_2 NMs (TiO_2 NPs and TiO_2 NTs) exhibited different adsorption, aggregation and sedimentation behavior in the presence of two different sources of HA. The adsorption of HA on the

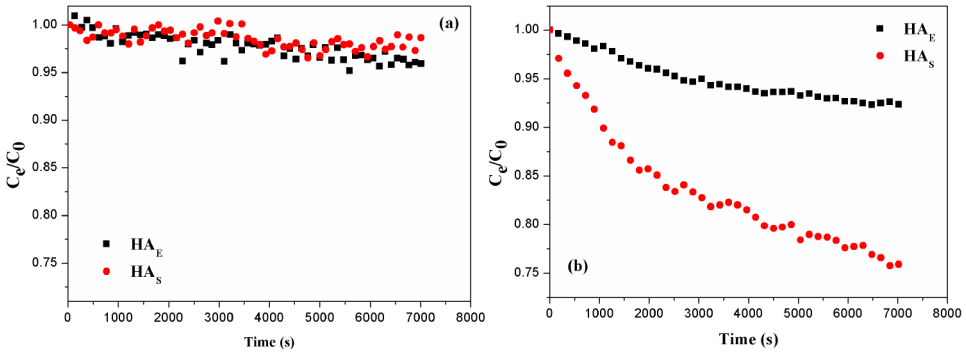

Fig. 7. Effect of sources of HA on the suspension/sedimentation performance of TiO_2 NPs (a) and TiO_2 NTs (b).

surfaces of TiO_2 NMs provides the basis for affecting the aggregation and sedimentation performance. Adsorption of HA on surface of TiO_2 NMs was driven by the combined action of electrostatic action, hydrophobic action, intermolecular force. The isoelectric point of TiO_2 NPs was greater than that of TiO_2 NTs. Therefore, TiO_2 NPs had a stronger electrostatic effect on HA adsorption under acidic conditions. Nonetheless, the adsorption percentage of HA_E on TiO_2 NPs and TiO_2 NTs were higher than that of HA_S under the same pH condition. The adsorption of HA_E and HA_S on TiO_2 NPs and HA_E on TiO_2 NTs were more inclined to be monolayer adsorption, TiO_2 NTs + HA_S might prefer multilayer adsorption. The adsorption of HA on TiO_2 NMs were better fitting pseudo second-order kinetics, the chemisorption was the main factor affecting the adsorption rate. As HA adsorbed on the surface of TiO_2 NMs, the suspension performance of TiO_2 NPs and TiO_2 NTs also increased, the solution pH, adsorption time, concentration of HA also influenced the suspension/sedimentation behavior of TiO_2 NPs and TiO_2 NTs, and aromatic-rich HA was found to have a greater stabilizing effect on TiO_2 NMs than aliphatic-rich HA.

Acknowledgements

This research was financially supported by the National Natural Science Foundation of China (No.41673131).

Appendix A. Supplementary data

Supplementary data to this article can be found online at https://doi.org/10.1016/j.scitotenv.2019.07.312.

References

Bavykin, D.V., Friedrich, J.M., Lapkin, A.A., Walsh, F.C., 2006. Stability of aqueous suspensions of titanate nanotubes. Chem. Mater. 18 (5), 1124–1129. https://doi.org/10.1021/cm0521875.

Chen, X.B., Mao, S.S., 2007. Titanium dioxide nanomaterials: synthesis, properties, modifications, and applications. Cheminform. 38 (41), 2891–2959. https://doi.org/10.1021/cr0500535.

Chen, Q., Du, G.H., Zhang, S., Peng, L.M., 2010. The structure of trititanate nanotubes. Acta. Crystallogr. B. 58 (4), 587–593. https://doi.org/10.1107/S0108768102009084.

Cheng, Y., Yang, H., Yang, Y., Huang, J.Y., Wu, K., Chen, Z., et al., 2018. Progress in TiO_2 nanotube coatings for biomedical applications: a review. J. Mater. Chem. B 6, 1862–1886. https://doi.org/10.1039/c8tb00149a.

Chowdhury, I., Cwiertny, D.M., Walker, S.L., 2012. Combined factors influencing the aggregation and deposition of nano-TiO_2 in the presence of humic acid and bacteria. Environ. Sci. Technol. 46 (13), 6968–6976. https://doi.org/10.1021/es2034747.

Dasari, T.P., Hwang, H.M., 2010. The effect of humic acids on the cytotoxicity of silver nanoparticles to a natural aquatic bacterial assemblage. Sci. Total Environ. 408 (23), 5817–5823. https://doi.org/10.1016/j.scitotenv.2010.08.030.

Erhayem, M., Sohn, M., 2014a. Stability studies for titanium dioxide nanoparticles upon adsorption of Suwannee River humic and fulvic acids and natural organic matter. Sci. Total Environ. 468-469, 249–257. https://doi.org/10.1016/j.scitotenv.2013.08.038.

Erhayem, M., Sohn, M., 2014b. Effect of humic acid source on humic acid adsorption onto titanium dioxide nanoparticles. Sci. Total Environ. 470-471, 92–98. https://doi.org/10.1016/j.scitotenv.2013.09.063.

Federici, G., Shaw, B.J., Handy, R.D., 2007. Toxicity of titanium dioxide nanoparticles to rainbow trout (*Oncorhynchus mykiss*): gill injury, oxidative stress, and other physiological effects. Aquat. Toxicol. 84 (4), 415–430. https://doi.org/10.1016/j.aquatox.2007.07.009.

Forgacs, E., Cserháti, T., Oros, G., 2004. Removal of synthetic dyes from wastewaters: a review. Environ. Int. 30 (7), 953–971. https://doi.org/10.1016/j.envint.2004.02.001.

Han, H., Song, T., Lee, E.K., Devadoss, A., Jeon, Y., Ha, J., et al., 2012. Dominant factors governing the rate capability of a TiO_2 nanotube anode for high power lithium ion batteries. ACS Nano 6 (9), 8308–8315. https://doi.org/10.1021/nn303002u.

Hillegass, J.M., Shukla, A., Lathrop, S.A., MacPherson, M.B., Fukagawa, N.K., Mossman, B.T., 2010. Assessing nanotoxicity in cells in vitro. Wires. Nanomed. Nanobi. 2 (3), 219–231. https://doi.org/10.1002/wnan.54.

Hochella, M.F., et al., 2019. Natural, incidental, and engineered nanomaterials and their impacts on the Earth system. Science 363 (6434), 1414–1424. https://doi.org/10.1126/science.aau8299.

Ji, Z.Q., Wu, R.L., Adamska, L., Velizhanin, K.A., Doorn, S.K., Sykora, M., 2014. In situ synthesis of graphene molecules on TiO_2: application in sensitized solar cells. ACS Appl. Mater. Interfaces 6 (22), 20473–20478. https://doi.org/10.1021/am506047f.

Kasuga, T., 2006. Formation of titanium oxide nanotubes using chemical treatments and their characteristic properties. Thin Solid Films 496 (1), 141–145. https://doi.org/10.1016/j.tsf.2005.08.341.

Kataoka, S., Gurau, M.C., Albertorio, F., Holden, M.A., Lim, S.M., Yang, R., et al., 2004. Investigation of water structure at the TiO_2/aqueous interface. Langmuir 20 (5), 1662–1666. https://doi.org/10.1021/la035971h.

Keller, A.A., Lazareva, A., 2014. Predicted releases of engineered nanomaterials: from global to regional to local. Environ. Sci. Technol. Lett. 1, 65–70. https://doi.org/10.1021/ez400106t.

Koo, M.S., Cho, K., Yoon, J., Choi, W., 2017. Photoelectrochemical degradation of organic compounds coupled with molecular hydrogen generation using electrochromic TiO_2 nanotube arrays. Environ. Sci. Technol. 51 (11), 6590–6598. https://doi.org/10.1021/acs.est.7b00774.

Lee, S., Kim, K., Shon, H.K., Kim, S.D., Cho, J., 2011. Biotoxicity of nanoparticles: effect of natural organic matter. J. Nanopart. Res. 13 (7), 3051–3061. https://doi.org/10.1007/s11051-010-0204-z.

Li, Y.J., Yang, C., Guo, X.T., Dang, Z., Li, X.Q., Zhang, Q., 2015. Effects of humic acids on the aggregation and sorption of nano-TiO_2. Chemosphere 119, 171–176. https://doi.org/10.1016/j.chemosphere.2014.05.002.

Lin, D.H., Ji, J., Long, Z.F., Yang, K., Wu, F.C., 2012. The influence of dissolved and surface-bound humic acid on the toxicity of TiO_2 nanoparticles to Chlorella sp. Water Res. 46 (14), 4477–4487. https://doi.org/10.1016/j.watres.2012.05.035.

Lin, D., Drew Story, S., Walker, S.L., Huang, Q.Y., Cai, P., 2016. Influence of extracellular polymeric substances on the aggregation kinetics of TiO_2 nanoparticles. Water Res. 104, 381–388. https://doi.org/10.1016/j.watres.2016.08.044.

Liu, A.H., Wei, M.D., Honma, I., Zhou, H.S., 2005. Direct electrochemistry of myoglobin in titanate nanotubes film. Anal. Chem. 77 (24), 8068–8074. https://doi.org/10.1021/ac051640t.

Liu, W., Sun, W.L., Borthwick, A.G.L., Ni, J.R., 2013. Comparison on aggregation and sedimentation of titanium dioxide, titanate nanotubes and titanate nanotubes-TiO_2: influence of pH, ionic strength and natural organic matter. Colloid. Surface. A. 434 (19), 319–328. https://doi.org/10.1016/j.colsurfa.2013.05.010.

Loosli, F., Le-Coustumer, P., Stoll, S., 2014. Effect of natural organic matter on the disagglomeration of manufactured TiO_2 nanoparticles. Environ. Sci-nano. 1 (2), 154–160. https://doi.org/10.1039/c3en00061c.

Lovern, S.B., Klaper, R., 2010. Daphnia magna mortality when exposed to titanium dioxide and fullerene (C60) nanoparticles. Environ. Toxicol. Chem. 25 (4), 1132–1137. https://doi.org/10.1897/05-278R.1.

Macak, J.M., Zlamal, M., Krysa, J., Schmuki, P., 2010. Self-organized TiO_2 nanotube layers as highly efficient photocatalysts. Small 3 (2), 300–304. https://doi.org/10.1002/smll.200600426.

Mcdonald, S., Bishop, A.G., Prenzler, P.D., Robards, K., 2004. Analytical chemistry of freshwater humic substances. Anal. Chim. Acta 527 (2), 105–124. https://doi.org/10.1016/j.aca.2004.10.011.

Mondal, B., Usha, K., Mahata, S., Kumbhakar, P., Nandi, M.M., 2011. Synthesis and characterization of nanocrystalline TiO_2 thin films for use as photoelectrodes in dye sensitized solar cell application. T. Indian. Ceram. Soc. 70 (3), 173–177. https://doi.org/10.1080/0371750X.2011.10600167.

Niu, H.Y., Wang, J.M., Shi, Y.L., Cai, Y.Q., Wei, F.S., 2009. Adsorption behavior of arsenic onto protonated titanate nanotubes prepared via hydrothermal method. Microporous Mesoporous Mater. 122 (1), 28–35. https://doi.org/10.1016/j.micromeso.2009.02.005.

Oberdoester, G., 2010. Nanotoxicology: An emerging discipline evolving from studies of ultrafine particles. Environ. Health. Persp. 118 (9), A380. https://doi.org/10.1289/ehp.1002354R.

Pan, B., Xing, B.S., 2008. Adsorption mechanisms of organic chemicals on carbon nanotubes. Environ. Sci. Technol. 42 (24), 9005–9013. https://doi.org/10.1021/es801777n.

Roy, P., Berger, S., Schmuki, P., 2011. TiO_2 nanotubes: synthesis and applications. Angew. Chem. Int. Ed. 50 (13), 2904–2939. https://doi.org/10.1002/anie.201001374.

Schnitzer, M., Khan, S.U., 1974. Humic substances in the environment. Soil Sci. Soc. Am. J. 117 (2), 130. https://doi.org/10.2136/sssaj1975.03615995003900030006x.

Sendra, M., Moreno-Garrido, I., Yeste, M.P., Gatica, J.M., Blasco, J., 2017. Toxicity of TiO_2, in nanoparticle or bulk form to freshwater and marine microalgae under visible light and UV-A radiation. Environ. Pollut. 227, 39–48. https://doi.org/10.1016/j.envpol.2017.04.053.

Shankar, K., Basham, J.I., Allam, N.K., Varghese, O.K., Mor, G.K., Feng, X.J., et al., 2009. Recent advances in the use of TiO_2 nanotube and nanowire arrays for oxidative photoelectrochemistry. J. Phys. Chem. C 113 (16), 6327–6359. https://doi.org/10.1021/jp809385x.

Sun, L., Perdue, E.M., Meyer, J.L., Weis, J., 1997. Use of elemental composition to predict bioavailability of dissolved organic matter in a Georgia river. Limnol. Oceanogr. 42 (4), 714–721. https://doi.org/10.4319/lo.1997.42.4.0714.

Supha, C., Boonto, Y., Jindakaraked, M., Ananpattarachai, J., Kajitvichyanukul, P., 2015. Long-term exposure of bacterial and protozoan communities to TiO_2 nanoparticles in an aerobic-sequencing batch reactor. Sci. Technol. Adv. Mater. 16 (3), 034609. https://doi.org/10.1088/1468-6996/16/3/034609.

Thio, B.J., Zhou, D., Keller, A.A., 2011. Influence of natural organic matter on the aggregation and deposition of titanium dioxide nanoparticles. J. Hazard. Mater. 189 (1), 556–563. https://doi.org/10.1016/j.jhazmat.2011.02.072.

Wang, Y.Q., Hu, G.Q., Duan, X.F., Sun, H.L., Xue, Q.K., 2002. Microstructure and formation mechanism of titanium dioxide nanotubes. Chem. Phys. Lett. 365 (5), 427–431. https://doi.org/10.1016/s0009-2614(02)01502-6.

Wang, J.X., Zhang, X.Z., Chen, Y.S., Sommerfeld, M., Hu, Q., 2008. Toxicity assessment of manufactured nanomaterials using the unicellular green alga Chlamydomonas reinhardtii. Chemosphere 73 (7), 1121–1128. https://doi.org/10.1016/j.chemosphere.2008.07.040.

Wang, Y., Gao, B., Morales, V.L., Tian, Y., Wu, L., Gao, J., et al., 2012. Transport of titanium dioxide nanoparticles in saturated porous media under various solution chemistry conditions. J. Nanopart. Res. 14 (9), 1–9. https://doi.org/10.1007/s11051-012-1095-y.

Xiong, L., Chen, C., Chen, Q., Ni, J.R., 2011. Adsorption of Pb(II) and Cd(II) from aqueous solutions using titanate nanotubes prepared via hydrothermal method. J. Hazard. Mater. 189 (3), 741–748. https://doi.org/10.1016/j.jhazmat.2011.03.006.

Zhang, Y., Chen, Y.S., Westerhoff, P., Crittenden, J., 2009. Impact of natural organic matter and divalent cations on the stability of aqueous nanoparticles. Water Res. 43 (17), 4249–4257. https://doi.org/10.1016/j.watres.2009.06.005.

Zhao, T.H., Tang, Z., Zhao, X.L., Zhang, H., Wang, J.Y., Wu, F.C., Giesy, J.P., Shi, J., 2019. Efficient removal of both antimonite (Sb(III)) and antimonate (Sb(V)) from environmental water using titanate nanotubes and nanoparticles. Environ. Sci.: Nano. 6, 834–850. https://doi.org/10.1039/C8EN00869H.

Zou, J.P., Liu, H.L., Luo, J.M., Xing, Q.J., Du, H.M., Jiang, X.H., Luo, X.B., Luo, S.L., Suib, S.L.L., 2016. Three-dimensional reduced graphene oxide coupled with Mn_3O_4 for highly efficient removal of Sb(III) and Sb(V) from water. ACS Appl. Mater. Interfaces 8, 18140–18149. https://doi.org/10.1021/acsami.6b05895 (2016).

Supporting Information （SI）

Adsorption, aggregation and sedimentation of titanium dioxide nanoparticles and nanotubes in the presence of different sources of humic acids

Tianhui Zhao[a,b], Mengyuan Fang[b,c], Zhi Tang[b,*], Xiaoli Zhao[b] , Fengchang Wu[b]

a. College of Water Sciences, Beijing Normal University, Beijing 100875, China.

b. State Key Laboratory of Environmental Criteria and Risk Assessment, Chinese Research Academy of Environmental Sciences, Beijing 100012, China.

c. Faculty of Environmental Science and Engineering, Kunming University of Science and Technology, Kunming Yunnan 650550, China

Corresponding author.

E-mail: tzwork@hotmail.com

Table S1 HA_E and HA_S compound constitution characteristics, element constitution and the relative content of each carbon containing group.

Carbon distribution (ppm)							
Sample	Carbonyl 220-190	Carboxyl 190-165	Aromatic 165-110	Acetal 110-90	Hetero Aliphatic 90-60	Aliphatic 60-0	Aromatic/ Aliphatic
HA_E	6	18	50	4	6	16	3.125
HA_S	6	15	31	7	13	29	1.069

Element constitution %（w/w）							
	H_2O	Ash	C	H	O	N	S	P
HA_E	8.2	0.88	58.13	3.68	34.08	4.14	0.44	0.24
HA_S	20.4	1.04	52.63	4.28	42.04	1.17	0.54	0.013

Acid functional groups （m mol/g）								
	Carboxyl	Phenolic	Q_1	$LogK_1$	N_1	Q_2	$LogK_2$	N_2
HA_E	8.28	1.87	8.90	4.36	3.16	0.85	9.80	1.00
HA_S	9.13	3.72	9.74	4.35	3.30	4.48	10.44	1.73

Data are reported from international Humic Substances Society (IHSS)

Table S2 Langmuir and Freundlich parameters for HA adsorption on the TiO_2 NPs and TiO_2 NTs.

Samples	Langmuir model			Freundlich model		
	q_m(mg/g)	k_L(L/mg)	R^2	n	k_F ($mg^{1-(1/n)}L^{1/n}/g$)	R^2
TiO_2 NPs+HA_E	236.05	0.04	0.974	1.60	15.97	0.964
TiO_2 NPs+HA_S	37.48	0.22	0.954	3.89	13.27	0.941
TiO_2 NTs+HA_E	146.05	0.06	0.902	2.00	17.32	0.868
TiO_2 NTs+HA_S	70.66	0.41	0.935	4.98	32.97	0.970

Table S3 Pseudo-first-order and Pseudo-second-order model Kinetics Constants for HA adsorption on the TiO_2 NPs and TiO_2 NTs.

Adsorbed types	Pseudo-second-order				Pseudo-first-order		
	K_2 g/mg/min)	q_e (mg/g)	h_0 (mg/g/min)	R^2	K_1	q_e (mg/g)	R^2
TiO_2 NPs+HA_E	5.60×10^{-4}	56.14	1.79	0.999	1.45×10^{-2}	54.00	0.782
TiO_2 NPs+HA_S	1.56×10^{-3}	23.95	0.89	0.997	1.16×10^{-2}	23.33	0.655
TiO_2 NTs+HA_E	2.84×10^{-4}	44.38	0.56	0.999	1.88×10^{-2}	39.00	0.585
TiO_2 NTs+HA_S	8.3×10^{-5}	29.03	0.07	0.985	0.28×10^{-2}	25.44	0.976

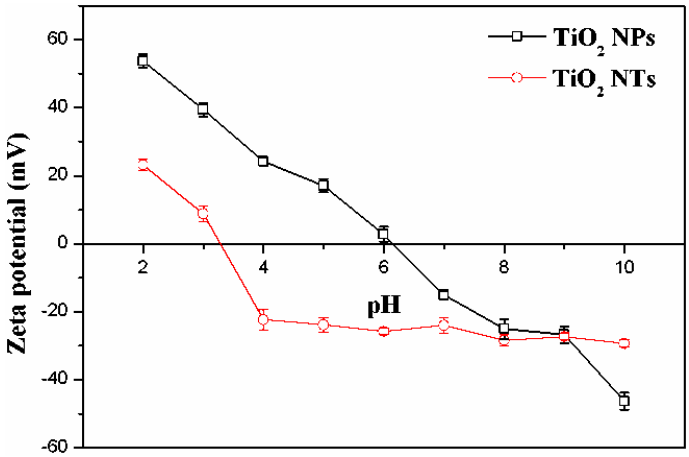

Fig. S1. The Zeta potential of TiO_2 NPs and TiO_2 NTs.

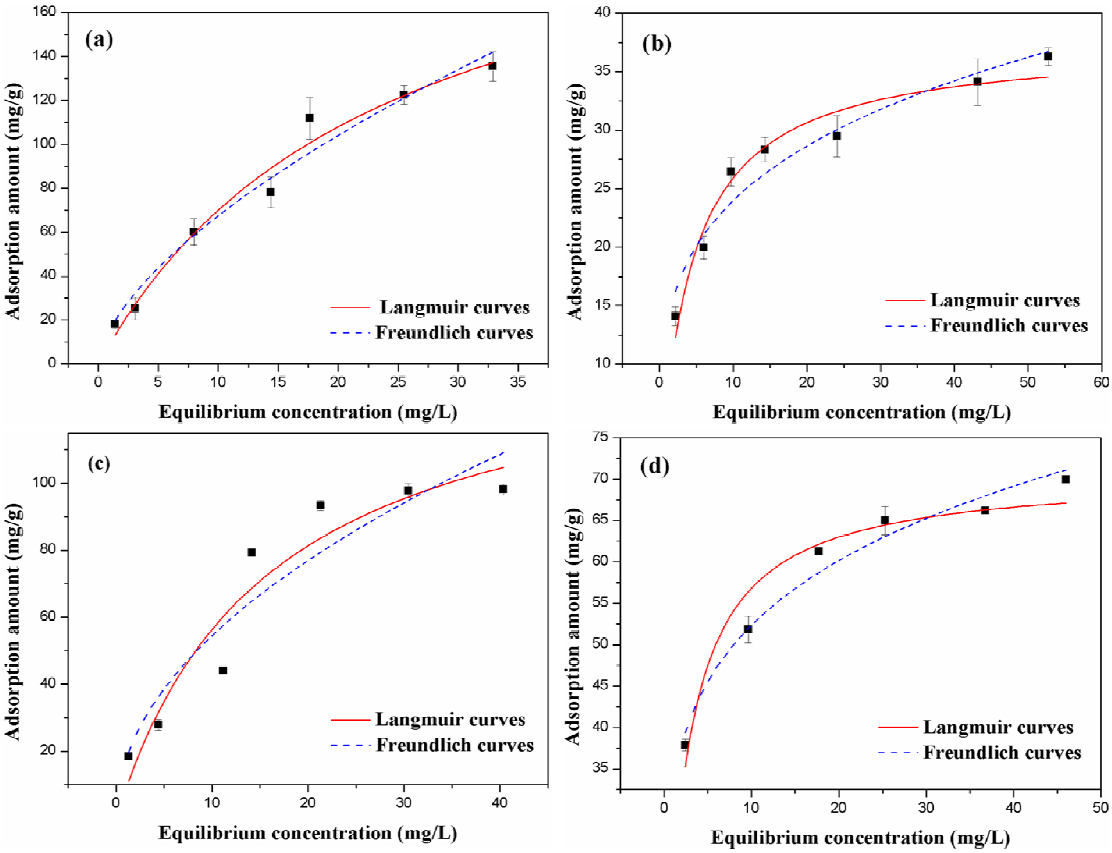

Fig. S2. Adsorption isotherm of HA_E on TiO_2 NPs (a), HA_S on TiO_2 NPs (b), HA_E on TiO_2 NTs (c) and HA_S on TiO_2 NTs (d).

The equilibrium adsorption isotherm data and related isotherm parameters were fitted using both Langmuir (eq 1) and Freundlich (eq 2) isotherm:

$$q_e = \frac{q_m k_L C_e}{1 + k_L C_e} \qquad (1)$$

$$q_e = k_F {C_e}^{1/n} \qquad (2)$$

Where: q_e is the amount (mg/g) of adsorbed HA at equilibrium and, Ce is the equilibrium HA concentration (mg/L) in solution. q_m (mg/g) represents the maximum adsorption capacity; k_L (L/g) is the Langmuir equilibrium constant; In Equation 2, k_F ($mg^{1-(1/n)}L^{1/n}/g$) and n are the Freundlich parameters.

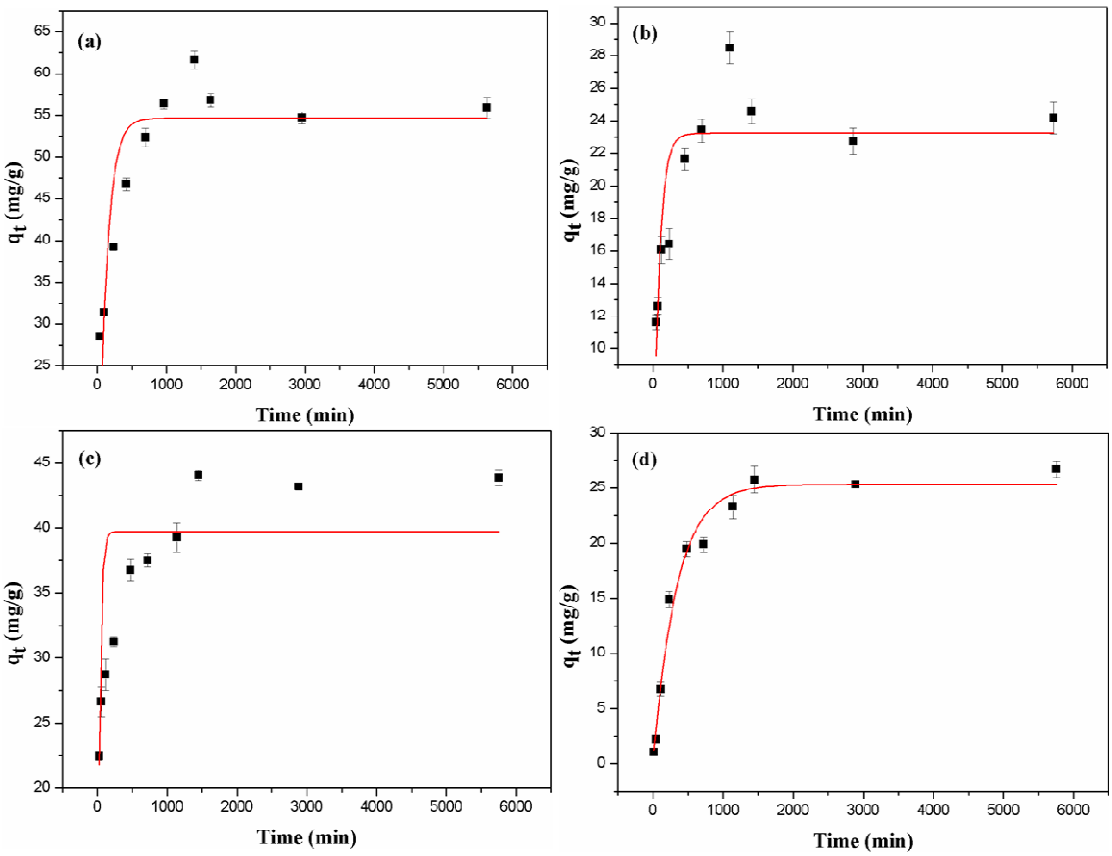

Fig. S3 First-order kinetics of TiO_2 NPs to HA_E (a) and HA_S (b), and TiO_2 NTs to HA_E (c) and HA_S (d).

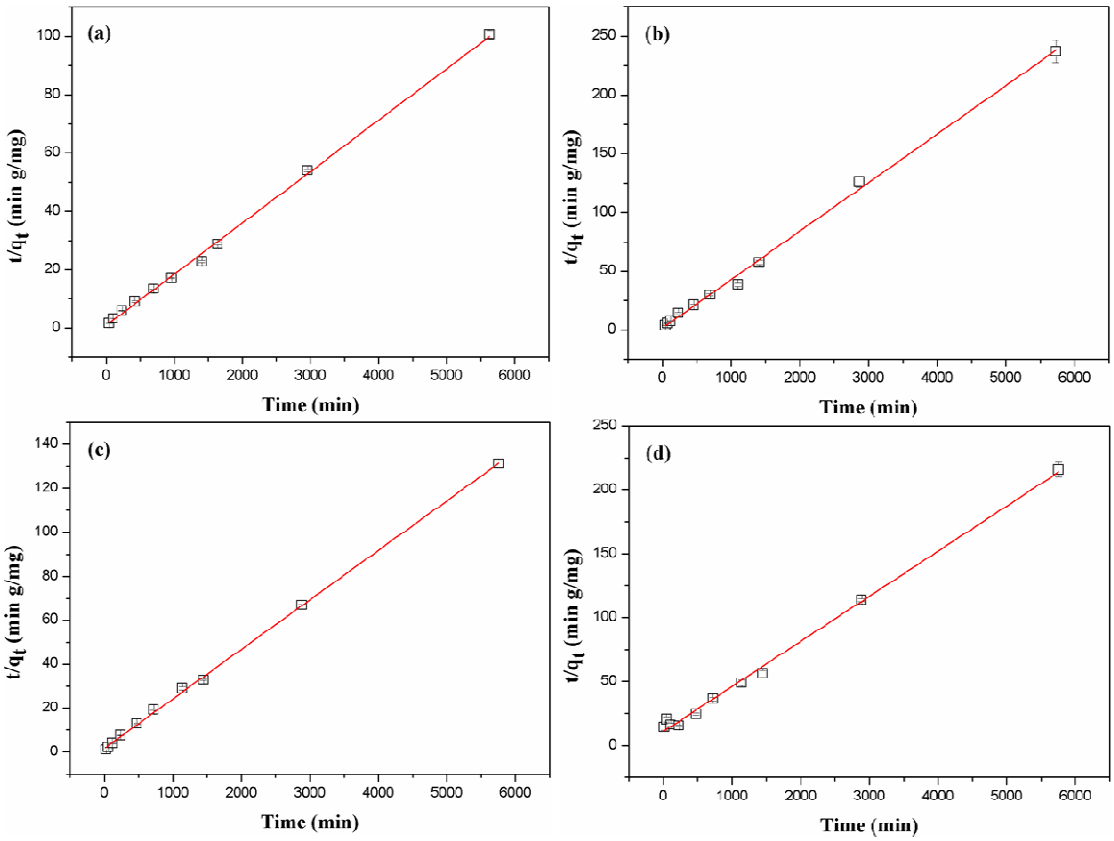

Fig. S4. Second-order kinetics of TiO_2 NPs to HA_E (a) and HA_S (b), and TiO_2 NTs to HA_E (c) and HA_S (d).

These fitted equations are shown in Equations 3-5. The fitting results are depicted in Figure S3 and S4, the relevant kinetic parameters are displayed in Table S3.

Pseudo-first-order kinetic models:

$$q_t = q_e(1 - e^{-K_1 t}) \quad (3)$$

Pseudo-second-order kinetic models:

$$\frac{t}{q_t} = \frac{1}{K_2 q_e^2} + \frac{1}{q_e} t \quad (4)$$

Where q_e is the amount of adsorbate at equilibrium (mg/g); q_t is the amount of adsorbate (mg/g) at time t (min); and K_1 (min^{-1}) and K_2 (g mg/min) are the rate

constants for the pseudo first-order and pseudo second-order sorption, respectively. Initial sorption rate, h_0 (mg/g/min) can be defined (Equation 5). K_2 and h_o can be extracted from the slope and intercept of a straight line obtained by mapping of t/q_t and t.

$$h_0 = K_2 q_e^2 \quad (t \to 0) \tag{5}$$